A 3D Segmentation Framework for Cornea Segmentation in Anterior Segment OCT Images using Level Set Technique with Shape Prior

Dominic Williams[1,2]
Yalin Zheng[2]
Fangjun Bao[3]
Ahmed Elsheikh[1]

[1] Ocular Biomechanics Group, University of Liverpool
[2] Department of Eye and Vision Science, University of Liverpool
[3] School of Optometry and Ophthalmology and Eye Hospital, Wenzhou Medical College

Abstract

Optical Coherence Tomography (OCT) images have the potential to provide quantitative measurements of the entire anterior segment of the eye. A new three-dimensional (3D) segmentation framework founded on level set based shape prior segmentation model has been developed for automatic segmentation of the entire cornea in 3D anterior segment OCT (AS-OCT). A three step algorithm was developed. The first step was to pre-process the image to reduce noise. The next step was to obtain a coarse segmentation of the front eye by using an entropy filter and the Otsu's thresholding technique. The final step used the new level set based shape prior segmentation model under cylindrical coordinates to evolve the contour initialised from the coarse segmentation and achieve the final segmentation. Initial results on synthetic image and real 3D AS-OCT images show promising results.

1. Introduction

Optical Coherence Tomography (OCT) is a non-invasive imaging technique. It has been used extensively on the retina at the back of the eye. The optically transparent nature of the human eye makes OCT a well suited imaging technique for retinal imaging [1]. There has been an increasing use of OCT to measure the geometry of the human cornea in vivo as well as anterior chamber biometry [2].

Anterior segment OCT (AS-OCT) is able to generate high speed and high resolution images of the front of the eye. It has widespread medical applications from contact lens fitting, modelling laser eye surgery to monitoring patients with eye pathologies [3]. In particular, obtaining accurate topography information of the anterior segment using this technique would also allow construction of patient-specific models for biomechanical modelling of the human eye [4]. There is currently a lack of automated measurement tools supplied with commercial OCT devices, and manual measurement is time consuming, tedious and subject to human errors. For this reason, there is an increasing need for fully automated segmentation techniques to accurately identify and trace both anterior and posterior boundaries of the anterior segment.

There have been several studies where segmentation of two-dimensional (2D) anterior segment OCT images has been explored [5, 6]. Williams et al have previously developed a 2D segmentation system for the anterior segment using a level set technique. Figure 1 shows an example 2D image segmented using their technique. In order to create a model of the entire cornea a three-dimensional (3D) segmentation technique is required. To the best of our knowledge, there is no approach that is able to segment the entire cornea in 3D anterior segment OCT images.

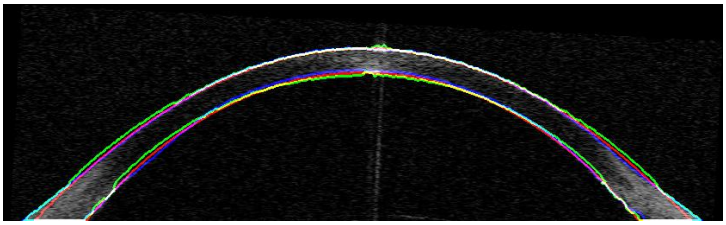

Figure 1: Example segmentation of 2D OCT image of cornea. Red line is CVWS, green line is CVWSe and blue line manual annotation. Colours are altered where lines overlap.

This study aims to develop a new segmentation framework that can automatically segment the cornea in 3D AS-OCT images. Due to the symmetric structure of the cornea, a series of cross-sectional images of the cornea all across the centre of the cornea but rotated relative to each other are taken to represent the cornea. Figure 2(a) demonstrates the scanning pattern and (b) illustrates the scan in the horizontal direction. For this specific problem it is envisaged that a new model using cylindrical polar coordinates will be more useful than conventional ones using Cartesian coordinates. Level set models can be extended to 3D without changing the energy function fundamentally. Previous work on 3D segmentation has mainly focused on models using Cartesian coordinates (ie a series of parallel scans of a subject being used to create a 3D image) [7]. One of the challenges in this work is the extension of previous 2D segmentation techniques to 3D using cylindrical polar coordinates and 3D shape prior.

This study aims to demonstrate the usability of level set using cylindrical coordinates for real applications represented by 3D cornea segmentation. The remainder of the paper is organised as follows. Section 2 describes the new segmentation framework in detail. Section 3 describes the experiments and presents the segmentation results. Section 4 discusses the results and concludes the paper.

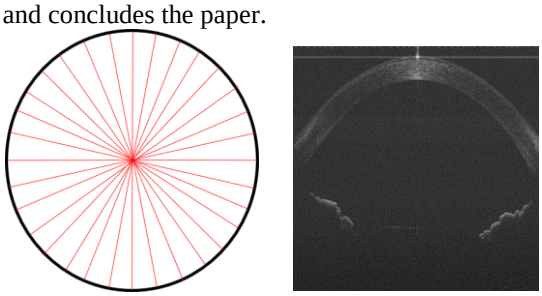

(a) (b)

Figure 2: Illustration of the 3D AS-OCT scanning pattern. (a) Diagram showing layout of radial scans. The black circle represents the cornea and each red line is a B scan of the cornea. Note only 16 scans are shown here for clarity. (b) An example scan in the horizontal direction. For the purpose of demonstration, the brightness and contrast has been adjusted.

2. Methods

2.1 3D AS-OCT

3D AS-OCT images using a customised AS-OCT device are used in this study. A typical 3D image dataset comprises 32 radial scans centred at the cornea with an angle of 11.25 degrees between. Each image section comprises 2048*2048 pixels corresponding to 12.05 mm and 7.71 mm in the horizontal and vertical direction respectively. Figure 2 shows the scanning pattern and a typical scan in the horizontal direction.

2.2 Segmentation Framework

A three step segmentation framework was developed. The first step was to pre-process the image to reduce noise. This involved using a combination of Gaussian filters and morphological processing to smooth noise from the image. A more advanced noise reduction method could have been used; however noise reduction was not the main focus or limiting factor in our segmentation technique. The next step was to obtain a coarse segmentation of the front eye by using entropy filter followed by the Otsu's thresholding technique. The final step used the new level set based shape prior segmentation model to evolve the contour initialised from the coarse segmentation and achieve the final segmentation.

2.2.1 Pre-processing step

The initial pre-processing step was to apply a Gaussian filter to the image. This acts to reduce the noise in the image, other filters could have been used such as median filter more suited to removing speckle noise. However the removal of noise was not the primary focus of this study and noise is not the limiting factor in improving results. Morphological processing was then used to remove some of the unwanted structures in the image. There was a tendency for bright horizontal bands to form above the cornea in the image, as can be seen in figure 2b. These were removed by morphological closing operation. Linear structural elements were used in this process.

2.2.2 Coarse Segmentation

The aim of this step is to produce an initial estimate of the corneal location (or coarse segmentation). This estimate is important as it will be used as the initial location of the curve to be evolved by the level set function in the following step, and also its anterior boundary will be used to construct the shape constraint in the later stage. Given the relatively good performance the technique described in [5] was adopted for this purpose. More specifically, an entropy filter was applied to the pre-processed image to produce an entropy map. The coarse segmentation is achieved by segmenting the entropy map using Otsu's thresholding method. This was applied image by image and the initial shape was assumed to be perfectly cylindrically symmetric.

2.2.3 Segmentation with Level Set and Shape Prior

A general segmentation model using level set and shape prior can be described as the following energy minimisation problem

$$E(\Phi(\boldsymbol{x}), c_1, c_2) = \lambda_1 \int_{\Omega} \delta\big(\Phi(\boldsymbol{x})\big)|\nabla\Phi(\boldsymbol{x})|d\boldsymbol{x} + \lambda_2^1 \int_{\Omega} (I(\boldsymbol{x}) - c_1)^2 H(\Phi) d\boldsymbol{x} + \lambda_2^2 \int_{\Omega} (I(\boldsymbol{x}) - c_2)^2 \big(1 - H(\Phi)\big) d\boldsymbol{x} \quad (1)$$

$$+\lambda_3 \int_{\Omega} (\Phi(\boldsymbol{x}) - S(\boldsymbol{x}))^2 d\boldsymbol{x}$$

$$+ \lambda_4 \int_{\Omega} (|\nabla\Phi| - 1)^2 \, d\boldsymbol{x}$$

where $\Phi(\boldsymbol{x})$ is the level set function, $\delta(\Phi)$ and $H(\Phi)$ are the delta function and Heaviside function respectively, $I(\boldsymbol{x})$ the image intensity, c_1 and c_2 the mean intensities inside and outside the zero level contour, and Ω the entire image volume. λs are the weighting parameters for different terms. In particular λ_2^1 and λ_2^2 can be used to apply different weights to the two region terms. $S(\boldsymbol{x})$ is a level set function corresponding to the shape prior. The first three terms in Eq (1) stands for the standard Chan and Vese's model [8]. The fourth term is a shape term that keeps $\Phi(\boldsymbol{x})$ close to the shape prior $S(\boldsymbol{x})$, the formulation of $S(\boldsymbol{x})$ will be detailed later. The last term is a regularisation form introduced by Li et al [9] to keep $\Phi(\boldsymbol{x})$ as a valid level set function without need of computationally expensive re-initialisation. The effect of this term is to penalise the formation of any regions with either very steep gradient or any flat areas.

The solution to Eq (1) can be derived by gradient descent approach as follows

$$\begin{aligned}\frac{\partial\Phi}{\partial t} = \; & \lambda_1 \, div\left(\frac{\nabla\Phi}{|\nabla\Phi|}\right) \delta(\Phi) - \lambda_2^1 \delta(\Phi)(Z(\boldsymbol{x}) - c_1)^2 + \lambda_2^2 (Z(\boldsymbol{x}) - c_2)^2 \\ & - 2\lambda_3 \big(\Phi(\boldsymbol{x}) - S(\boldsymbol{x})\big) + \lambda_4 (\nabla^2\Phi - div\left(\frac{\nabla\Phi}{|\nabla\Phi|}\right))\end{aligned} \tag{2}$$

The energy function was minimised by alternatively minimising Φ, c_1 and c_2. When Φ is fixed, the terms c_1 and c_2 using the following expressions

$$c_1 = \frac{\int_{\Omega} Z(\boldsymbol{x}) H(\Phi(\boldsymbol{x})) d\boldsymbol{x}}{\int_{\Omega} H(\Phi(\boldsymbol{x})) d\boldsymbol{x}} \tag{3}$$

$$c_2 = \frac{\int_{\Omega} Z(\boldsymbol{x})(1 - H(\Phi(\boldsymbol{x}))) d\boldsymbol{x}}{\int_{\Omega} (1 - H(\Phi(\boldsymbol{x}))) d\boldsymbol{x}} \tag{4}$$

In the iterations, the shape prior ***S(x)*** was also updated. An ellipsoid was estimated by least square fitting of the top surface of the level set function. A second related ellipsoid was built at a fixed distance below the first one. The shape prior of the cornea ***S(x)*** was then computed as the product of the level set functions corresponding to those two ellipsoids.

$$S(\boldsymbol{x}) = S_{upper}(\boldsymbol{x}) \, S_{lower}(\boldsymbol{x}) \tag{5}$$

where $S_{upper}(\boldsymbol{x})$ is a signed distance function corresponding to ellipsoid fitted to top surface and $S_{lower}(\boldsymbol{x})$ corresponds to a related ellipsoid which has been shifted down to mimic the lower surface of the cornea. Taking the product ensures a sign difference between the volume between the ellipsoids and outside the ellipsoids. This was performed once every 100 iterations in order to speed up the program.

In the discretisation the main difference between cylindrical and Cartesian coordinate is the curvature term: the former one is more complex. More specifically, the curvature under cylindrically polar coordinate becomes

$$div\left(\frac{\nabla\Phi}{|\nabla\Phi|}\right) = \frac{1}{r}\frac{\partial}{\partial r}\left(\frac{r\,\Phi_r}{|\nabla\Phi|}\right) + \frac{1}{r}\frac{\partial}{\partial\theta}\left(\frac{1}{r}\Phi_\theta \frac{1}{|\nabla\Phi|}\right) + \frac{\partial}{\partial z}\left(\Phi_z \frac{1}{|\nabla\Phi|}\right) \tag{6}$$

where r, θ and z are cylindrical coordinates. This was implemented using central difference approximations for the partial differentials in 3D.

The level set function $\Phi(\boldsymbol{x})$ was updated until either the update had only a very small effect on the position of contour or 2,000 iterations were reached.

3. Results

The new segmentation framework was tested on a synthetic image and a real 3D AS-OCT image. During the tests the constants determining the strength of different components of energy were empirically chosen for the best results. The values for the different constants used are $\lambda_1 = 0.2$, $\lambda_2^1 = \lambda_2^2 = 1$, $\lambda_3 = 0.8$ and $\lambda_4 = 0.1$.

A synthetic volume data was built using two ellipsoids with different radii to model the cornea. In each section some regions were deleted deliberately to simulate the OCT data where some regions are missing due to poor signal to noise ratio. Speckle noise was also added to these images since speckle noise is present in OCT data. Figure 3(a) shows the synthetic data in montage form of all 32 sections. Figure 3(b) shows the segmentation results. It can be seen that the new segmentation framework is capable of recovering the artificial gaps we have put in our 'cornea' to model areas of lower signal found in real data.

The program was also tested on a single 3D OCT image of the human cornea, see Figure 4(a). The image was taken from a healthy normal eye using a customised spectral domain OCT machine. There are 32 cross-sectional scans of the cornea were taken with the scan being rotated 11.25 degrees between each image. Figure 4(b) shows the segmentation result on Figure 4(a). It can be seen from this that our program can satisfactorily segment the cornea.

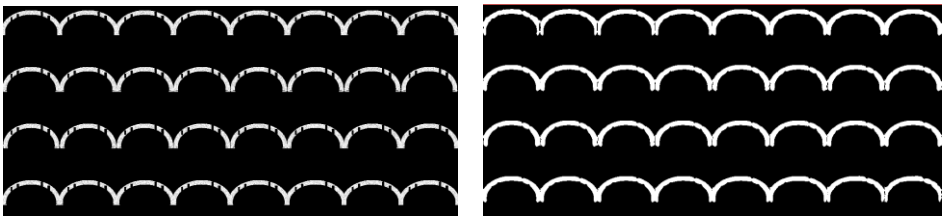

Figure 3: A synthetic image and its segmentation result. (a) Synthetic data with 32 images arranged in a radial pattern; (b) Segmentation result of the image in (a).

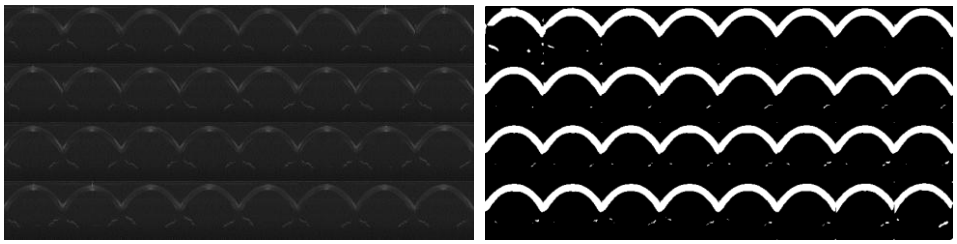

Figure 4: Illustration of segmentation of a 3D AS-OCT image. (a) A 3D OCT image of the human cornea where 32 images shown here are arranged in a radial pattern to give the 3D image of the cornea; (b) Segmented cornea in the image (a).

4. Conclusion

A fully automatic 3D segmentation framework using level set model with shape prior has been developed. It is capable of segmenting 3D images of the cornea using cylindrically polar coordinates. The usability of this model was assessed using synthetic data and real 3D AS-OCT images. Our preliminary results showed that the framework can achieve satisfactory results even though some regions in the image has very low signal to noise ratio for which conventional segmentation without shape prior is unlikely to succeed. To the best of our knowledge this is the first paper presenting results on 3D segmentation of the cornea in 3D AS-OCT images.

Future work is to optimise the framework for speed by improving the computational efficiency. This could be achieved by implementing it using graph cut technique. Moreover, further validation will also be performed against manual segmentation on a large dataset of OCT images. It is hoped that the results of this segmentation will eventually be used as an input in patient specific biomechanical modelling of the human eye.

5. References

[1] E. A. Swanson, J. A. Izatt, M. R. Hee, D. Huang, C. P. Lin, J. S. Schuman, C. A. Puliafito, and J. G. Fujimoto, "In vivo retinal imaging by optical coherence tomography," *Opt. Lett.*, vol. 18, pp. 1864-1866, 1993.

[2] B. J. Kaluzy, J. J. Kałuzny, A. Szkulmowska, I. Gorczyńska, M. Szkulmowski, T. Bajraszewski, M. Wojtkowski, and P. Targowski, "Spectral optical coherence tomography: A novel technique for cornea imaging," *Cornea*, vol. 25, pp. 960-965, 2006.

[3] L. M. Sakata, R. Lavanya, D. S. Friedman, H. T. Aung, H. Gao, R. S. Kumar, P. J. Foster, and T. Aung, "Comparison of gonioscopy and anterior segment ocular coherence tomography in detecting angle closure in different quadrants of the anterior chamber angle," *Ophthalmology*, vol. 115, pp. 769-774, 2008.

[4] A. Elsheikh and D. Wang, "Numerical modelling of corneal biomechanical behaviour," *Computer Methods in Biomechanics and Biomedical Engineering*, vol. 10, pp. 85-95, 2007.

[5] M. Shen, L. Cui, M. Li, D. Zhu, M. R. Wang, and J. Wang, "Extended scan depth optical coherence tomography for evaluating ocular surface shape," *Journal of Biomedical Optics*, vol. 16, 2011.

[6] D. Williams, Y. Zheng, F. Bao, and A. Elsheikh, "Automatic segmentation of anterior segment optical coherence tomography images," *Journal of Biomedical Optics*, vol. 18, pp. 056003-056003, 2013.

[7] J. Yang and J. S. Duncan, "3D image segmentation of deformable objects with joint shape-intensity prior models using level sets," *Medical Image Analysis*, vol. 8, pp. 285-294, 2004.

[8] T. F. Chan and L. A. Vese, "Active contours without edges," *IEEE Transactions on Image Processing*, vol. 10, pp. 266-277, 2001.

[9] C. Li, C. Xu, C. Gui, and M. D. Fox, "Level set evolution without re-initialization: a new variational formulation," 2005, pp. 430- 436 vol. 1-430- 436 vol. 1.